Scheme IV

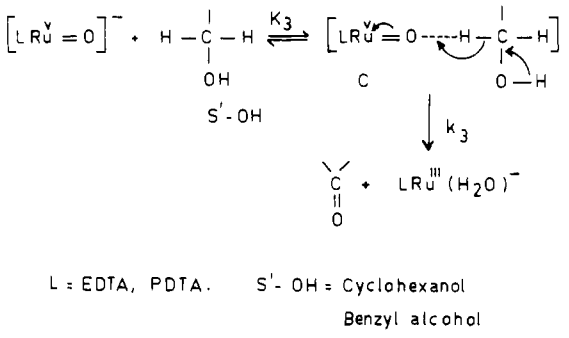

L = EDTA, PDTA. S'-OH = Cyclohexanol, Benzyl alcohol

The reaction with toluene did not give any nuclear hydroxylation products.

Kinetics of Oxidation of Cyclohexanol and Benzyl Alcohol with $LRu^{V}=O^{-}$. The oxidation of cyclohexanol to cyclohexanone and benzyl alcohol to benzaldehyde was studied further, as trace amounts of cyclohexanone and benzaldehyde were obtained as reaction products in the oxidation of cyclohexane and toluene by $LRu^{V}=O^{-}$. The rate of oxidation of the alcohol (cyclohexanol, benzyl alcohol) was first order with respect to the concentration of oxo complex $LRu^{V}=O^{-}$. Increase of alcohol concentration increased the reaction rate, and at high alcohol concentration the reaction rate became independent of alcohol concentration; i.e., saturation in rate was attained. On the basis of the above experimental facts, a mechanism for the oxidation of cyclohexanol to cyclohexanone and benzyl alcohol to benzaldehyde is proposed in Scheme IV, for which the rate expression is given in eqs 11 and 12.

$$k_{3(obs)} = \frac{k_3K_3[S'OH]}{1 + K_3[S'OH]} \quad (18)$$

or

$$\frac{1}{k_{3(obs)}} = \frac{1}{k_3} + \frac{1}{k_3K_3[S'OH]} \quad (19)$$

The values of k_3 calculated by using eq 19 are summarized in Table III.

In the suggested mechanism, the oxo oxygen of $LRu^{V}=O^{-}$ first attacks the C-H bond in alcohol to give rise to an intermediate "C", which in turn rearranges in a rate-determining step to give cyclohexanone or benzaldehyde as the reaction product. The major energetic factor here is the formation of the carbonyl group. The oxidation of cyclohexanol to cyclohexanone and benzyl alcohol to benzaldehyde was studied at three different temperatures, and the rate and activation parameters ($\Delta H^{\ddagger}$ and $\Delta S^{\ddagger}$) are presented in Table III.

Oxidation of the cyclic ether tetrahydrofuran with $LRu^{V}=O^{-}$ was carried out under experimental conditions identical with those described for olefin epoxidation and oxidation of a saturated substrate. The rate and activation parameters are presented in Table III. It is of interest to note that no hydroxylated intermediate of tetrahydrofuran could be detected during the product analysis. Hence, it is assumed that the very reactive γ-hydroxytetrahydrofuran if formed in the reaction mixture during oxidation of tetrahydrofuran with $LRu^{V}=O$ rearranges itself rapidly to the stable γ-butyrolactone as the ultimate reaction product.

Registry No. $K[Ru^{III}(EDTA\text{-}H)Cl]$, 76095-13-1; $K[Ru^{III}(PDTA\text{-}H)Cl]$, 141271-84-3; $K[Ru^{III}(EDTA\text{-}H)Cl]\cdot 2H_2O$, 141248-95-5; $K[Ru^{III}(PDTA\text{-}H)Cl]\cdot 0.5H_2O$, 141271-82-1; $Ru^{III}(EDTA)(OH)^{2-}$, 66844-68-6; $Ru^{III}(PDTA)(OH)^{2-}$, 141248-96-6; $K[Ru^{V}=O(EDTA)]\cdot 3H_2O$, 141248-97-7; $K[Ru^{V}=O(PDTA)]\cdot 3H_2O$, 141271-83-2; cyclohexene, 110-83-8; cyclooctene, 931-88-4; styrene, 100-42-5; *cis*-stilbene, 645-49-8; *trans*-stilbene, 103-30-0; cyclohexane, 110-82-7; tetrahydrofuran, 109-99-9; 2-Me-styrene, 611-15-4; 3-Cl-styrene, 2039-85-2; 4-MeO-styrene, 637-69-4; cyclohexene oxide, 286-20-4; cyclooctene oxide, 286-62-4; styrene oxide, 96-09-3; 2-Me-styrene oxide, 2783-26-8; 3-Cl-styrene oxide, 20697-04-5; 4-MeO-styrene oxide, 6388-72-3; *cis*-stilbene oxide, 1689-71-0; *trans*-stilbene oxide, 1439-07-2; cyclohexanol, 108-93-0; cyclohexanone, 108-94-1; benzyl alcohol, 100-51-6; benzaldehyde, 100-52-7; γ-butyrolactone, 96-48-0.

Supplementary Material Available: Tables of positional parameters, general displacement parameter expressions, bond distances, least-squares planes, and torsional angles (18 pages); listings of observed and calculated structure factors (20 pages). Ordering information is given on any current masthead page.

Contribution from the Department of Chemistry and Laboratory for Molecular Structure and Bonding, Texas A&M University, College Station, Texas 77843-3255, and Department of Chemistry, University of Costa Rica, Ciudad Universitaria, Costa Rica

Mononuclear-Dinuclear Equilibrium for the Pyridine Adducts of Chromium(II) Saccharinates

Nuria M. Alfaro,[1a] F. Albert Cotton,*[1b] Lee M. Daniels,[1b] and Carlos A. Murillo*[1a]

Received January 17, 1992

The azeotropic removal of water by pyridine from $[Cr(Sac)_2(H_2O)_4]\cdot 2H_2O$, Sac = the anion of saccharine, gives a solution with a mixture of a mononuclear and dinuclear chromium(II) saccharinate, the relative concentration of which varies with changes in temperature. Appropriate workup of the pyridine solution has provided crystals of $[Cr_2(Sac)_4(py)_2]\cdot 2py$ (**1**) and $[Cr(Sac)_2(py)_3]\cdot 2py$ (**2**). Both compounds have been characterized by X-ray crystallography at −60 °C. The chromium-to-chromium bond length in **1** (2.5911 (8) Å) is one of the longest ones known of any dichromium(II) dimer. Compound **1** crystallizes in the monoclinic space group *Ia*, with a = 11.705 (2) Å, b = 21.868 (2) Å, c = 20.649 (2) Å, β = 98.87 (1)°, V = 5222 (2) Å^3, and Z = 4. The structure of the five-coordinated compound **2** is bipyramidal and is easily envisioned as the result of breaking the metal-to-metal bond in **1** and replacing the O-bonded saccharinate groups by pyridine molecules. Compound **2** crystallizes in the monoclinic space group $C2/c$, with a = 13.347 (2) Å, b = 26.134 (2) Å, c = 11.802 (2) Å, β = 110.541 (7)°, V = 3855 (1) Å^3, and Z = 4. Both compounds possess interstitial pyridine molecules that occupy channels formed in the crystal. Under appropriate conditions **1** and **2** are reversibly interconvertable both in the solid state and in pyridine solution.

Introduction

The chemistry of chromium(II) is very rich in mononuclear six-coordinated compounds, most of them having the high-spin electronic configuration. One point of particular interest has been the Jahn-Teller distortion exhibited by these compounds.[2] There is also a more limited number of four-coordinated species, either nearly planar or tetrahedral,[3] and a few reports of three- and five-coordinated compounds.[4] To our knowledge, there is only

(1) (a) University of Costa Rica. (b) Texas A&M University.
(2) Cotton, F. A.; Wilkinson, G. *Advanced Inorganic Chemistry*, 5th ed.; John Wiley & Sons: New York, 1988; Chapter 18, pp 683-686.
(3) See for example: (a) Bradley, D. C.; Hursthouse, M. B.; Newing, C. W.; Welch, A. J. *J. Chem. Soc., Chem. Commun.* **1972**, 567. (b) Cotton, F. A.; Falvello, L. R.; Schwotzer, W.; Murillo, C. A.; Valle-Bourrouet, G. *Inorg. Chim. Acta* **1991**, *190*, 89 and references cited therein.

0020-1669/92/1331-2718$03.00/0

one single-crystal diffraction study of a square-pyramidal chromium(II) species reported so far,[5] although five-coordination has been assumed for other compounds, such as [CrN-$(CH_2CH_2NMe_2)_3$Br]Br, which was shown by X-ray powder studies to be isomorphous with the bipyramidal Co analog.[6] A series of other chromium(II) complexes bonded to tripod ligands has also been shown, by spectroscopic studies, to have five-coordination of the metal center.[7]

Another area of interest in the chemistry of chromium(II) is that of the formation of dichromium species,[8] in some of which there are very short metal-to-metal separations (less than 2.0 Å) as well as rather long ones (ca. 2.5 Å).

In our laboratories, we have been studying the effect of different variables on Cr(II) Jahn–Teller active species.[9] The saccharinate anion has been used in several of our investigations, and we have shown that it is capable of producing either mononuclear[9a,b] or dinuclear compounds when it reacts with chromium(II) species. The THF adduct of the dinuclear complex[9a] has a very long metal-to-metal bond, namely 2.550 Å, but remains intact. However, when pyridine was used as solvent, we observed a monomer–dimer equilibrium and therefore decided to investigate this system further.

Experimental Section

All operations were carried out under a nitrogen atmosphere using standard Schlenk techniques. Solvents were dried, deoxygenated, and distilled just before they were used. UV–vis spectra were obtained in a Shimadzu UV-160 spectrometer equipped for variable-temperature studies. Pyridine analysis was performed by measuring the weight loss after heating the samples under a vacuum. The chromium content was determined as Cr_2O_3, after samples were hydrolyzed and calcinated. Saccharine was determined by a published method[10] after the compounds were acid-hydrolyzed, and then it was extracted with diethyl ether. Satisfactory analyses were obtained.

Azeotropic Distillation of Water. In a typical experiment, 50 mL of pyridine was added to crystalline $[Cr(Sac)_2(H_2O)_4]\cdot 2H_2O$[11] (0.90 g, 1.70 mmol). After brief stirring at room temperature, a brownish solution was formed. Then, 20 mL of solvent was distilled away. While hot, the solution was green, but the color changed to brown when it was allowed to return to room temperature.

$[Cr_2(Sac)_4(py)_2]\cdot 2py$ (1). To 8 mL of the above solution was carefully added a layer of 10 mL of hexane, and the mixture was left at 25 °C. Red single crystals slowly grew near the interface of the two liquid phases. If the hexane was allowed to diffuse completely, essentially quantitative yields were obtained.

The product was also obtained, in a microcrystalline form, by addition of hexane and then mixing the two liquid phases by slow swirling of the flask. Filtration and washing with two 10-mL portions of hexane gave a near 100% yield.

$[Cr(Sac)_2(py)_3]\cdot 2py$ (2). This compound was prepared in an analogous way to **1**, but the temperature of the two phase mixture was kept at −10 °C. Very long needlelike green crystals grew in nearly quantitative yields.

Mixtures of Crystals. Crystals of both **1** and **2** were formed when the above mixture was kept at 10 °C or when the chromium(II) saccharinate solution was cooled to 0 °C before the addition of hexane and then the mixture was allowed to stand at room temperature.

Table I. Crystal Data for $[Cr_2(Sac)_4(py)_2]\cdot 2py$ and $[Cr(Sac)_2(py)_3]\cdot 2py$

formula	$Cr_2S_4O_{12}N_8C_{48}H_{36}$	$CrS_2O_6N_7C_{39}H_{33}$
fw	1149.12	811.87
space group	*Ia*	*C2/c*
a, Å	11.705 (2)	13.347 (2)
b, Å	21.868 (2)	26.134 (2)
c, Å	20.649 (2)	11.802 (2)
β, deg	98.87 (1)	110.541 (7)
V, Å^3	5222 (2)	3855 (1)
Z	4	4
d_{calcd}, g/cm^3	1.461	1.399
μ(Mo Kα), cm^{-1}	6.242	4.461
radiation (monochromated in incident beam)	Mo Kα (λ_α = 0.710 73 Å)	
temp, °C	−60 (1)	−60 (1)
transm factors: max; min	0.9990, 0.9130	0.9985, 0.9645
R^a	0.033	0.057
R_w^b	0.049	0.086

$^a R = \sum||F_o| - |F_c||/\sum|F_o|$. $^b R_w = [\sum w(|F_o| - |F_c|)^2/\sum w|F_o|^2]^{1/2}$; $w = 1/\sigma^2(|F_o|)$.

Crystallographic Studies. For both **1** and **2** geometric and intensity data were taken on an Enraf-Nonius CAD-4 diffractometer by employing procedures described previously.[12]

An orange-red crystal of **1** was mounted on the tip of a glass fiber with its longest axis approximately aligned with the fiber and quickly moved into the cold stream of the low-temperature device. The data were corrected for Lorentz and polarization effects, and an absorption correction based on a series of ψ-scans was applied. The value of $R_{int}(F_o)$ based on the averaging of 470 observed reflections was 0.009.

Because of the similarity of the unit cell to that of the homologous complex $Cr_2(Sac)_4(THF)_2$,[3b] the initial attempt to solve the structure was made in the centric space group *I2/a* using the coordinates of that homologue. However, no reasonable refinement was possible, and no reasonable solutions were found from either a Patterson map or direct methods. The correct solution came immediately from direct methods in the noncentric space group *Ia* (a nonstandard setting of space group No. 9). Following full-matrix least-squares refinement of the metal complex, a difference map revealed two independent molecules of pyridine in the lattice. While the metal complex approximately retains the 2-fold symmetry of the THF homologue, the positions of the interstitial pyridine molecules preclude the presence of crystallographic 2-fold axes or inversion centers.

The relatively large thermal parameters for the interstitial pyridine molecules frustrated any attempt to determine the position of the nitrogen atom in each ring, assuming that the molecules are indeed ordered. Systematic assignment of nitrogen scattering factors to one atom in each ring followed by least-squares refinement cycles provided no hint as to the true position of the nitrogen atom. The atoms of the interstitial solvent molecules were therefore all refined as carbon atoms.

In the final stages of refinement, all non-hydrogen atoms of the metal complex were refined with anisotropic thermal parameters, while the interstitial solvent molecules were left to refine isotropically. Hydrogen atoms were used in idealized positions on the coordinated ligands for the calculation of the structure factors only.[13]

A green crystal of **2** was mounted on the tip of a glass fiber with its longest axis approximately aligned with the fiber and quickly moved into the cold stream of the low-temperature device. The data were corrected for Lorentz and polarization effects, and an absorption correction based on a series of ψ-scans was applied. The value of $R_{int}(F_o)$ based on the averaging of 291 observed reflections was 0.015.

The presence of the *c*-glide plane was unambiguously indicated by the systematic absences. The choice of the centric space group *C2/c* was favored by intensity statistics and was verified by the successful refinement of the model. A model representing all 23 of the unique non-hydrogen atoms of the complex was constructed from the peaks in a direct-methods *E*-map, in which the Cr atom and one of the pyridine ligands reside on the crystallographic 2-fold axis. Following several cycles

(4) Larkworthy, L. F.; Nolan, K. B.; O'Brien, P. In *Comprehensive Coordination Chemistry*; Wilkinson, G., Guillard, R. D., McCleverty, J. A., Eds.; Pergamon Press: Oxford, England, 1987; Vol. 3, Chapter 35, p 702.
(5) Edema, J. J. H.; Gambarotta, S.; Meetsma, A.; van Bolhuis, F.; Spek, A. L.; Smeets, W. J. *J. Inorg. Chem.* **1990**, *29*, 2147.
(6) Ciampolini, M. *Chem. Commun.* **1966**, 47.
(7) (a) Mani, F.; Stoppioni, P. *Inorg. Chim. Acta* **1976**, *16*, 177. (b) Mani, F.; Stoppioni, P.; Sacconi, L. *J. Chem. Soc., Dalton Trans.* **1975**, 461. (c) Mani, F.; Sacconi, L. *Inorg. Chim. Acta* **1970**, *4*, 365. (d) Ciampolini, M.; Nardi, N. *Inorg. Chem.* **1966**, *5*, 1150.
(8) (a) Cotton, F. A.; Walton, R. A. *Multiple Bonds Between Metal Atoms*, 1st ed.; John-Wiley & Sons: New York, 1982; Chapter 4. (b) *Ibid.*, 2nd ed., in press.
(9) (a) Cotton, F. A.; Lewis, G. E.; Murillo, C. A.; Schwotzer, W.; Valle, G. *Inorg. Chem.* **1984**, *23*, 4038. (b) Cotton, F. A.; Falvello, L. R.; Murillo, C. A.; Valle, G. *Z. Anorg. Allg. Chem.* **1986**, *540/541*, 67. (c) Cotton, F. A.; Falvello, L. R.; Ohlhausen, E. L.; Murillo, C. A.; Quesada, J. F. *Z. Anorg. Allg. Chem.* **1991**, *599/600*, 55. (d) Cotton, F. A.; Falvello, L. R.; Murillo, C. A.; Quesada, J. F. *J. Solid State Chem.* **1992**, *96*, 192.
(10) *The US Pharmacopeia*, 21st ed.; United States Pharmacopeial Convention, Inc.: Rockville, MD, 1985.
(11) Cotton, F. A.; Libby, E.; Murillo, C. A.; Valle, G. *Inorg. Synth.* **1990**, *27*, 306.
(12) Bino, A.; Cotton, F. A.; Fanwick, P. E. *Inorg. Chem.* **1979**, *18*, 3558.
(13) Refinement calculations were carried out on a local area VAX cluster using the SHELX-76 programs.

Table II. Positional Parameters and B Values and Their Estimated Standard Deviations for $[Cr_2(Sac)_4(py)_2]\cdot 2py$[a]

atom	x	y	z	B, Å^2	atom	x	y	z	B, Å^2
Cr(1)	0.750	0.17863 (2)	0.500	1.890 (9)	C(14)	0.6135 (4)	0.3211 (2)	0.7008 (2)	2.80 (8)
Cr(2)	0.74142 (5)	0.29602 (2)	0.48290 (3)	1.955 (9)	C(15)	0.5245 (3)	0.2188 (2)	0.4478 (2)	2.23 (7)
S(1)	1.01596 (8)	0.34482 (4)	0.51991 (5)	2.64 (2)	C(16)	0.3986 (3)	0.2158 (2)	0.4264 (2)	2.77 (7)
S(2)	0.64772 (9)	0.15441 (4)	0.63963 (5)	2.57 (2)	C(17)	0.3493 (4)	0.2727 (2)	0.4196 (2)	3.09 (8)
S(3)	0.46030 (9)	0.32747 (5)	0.43756 (5)	2.81 (2)	C(18)	0.2313 (4)	0.2817 (3)	0.4008 (3)	4.4 (1)
S(4)	0.84942 (9)	0.12090 (4)	0.36881 (5)	2.60 (2)	C(19)	0.1647 (4)	0.2291 (3)	0.3894 (3)	5.2 (1)
O(1)	0.9160 (2)	0.1869 (1)	0.5438 (1)	2.36 (5)	C(20)	0.2121 (4)	0.1711 (3)	0.3962 (3)	5.0 (1)
O(2)	1.0299 (3)	0.3608 (2)	0.4545 (2)	3.81 (6)	C(21)	0.3309 (4)	0.1634 (2)	0.4144 (3)	3.58 (9)
O(3)	0.9908 (3)	0.3926 (1)	0.5625 (2)	3.94 (7)	C(22)	0.8089 (3)	0.2323 (2)	0.3741 (2)	2.28 (7)
O(4)	0.7091 (2)	0.3067 (1)	0.5748 (1)	2.38 (5)	C(23)	0.8570 (3)	0.2247 (2)	0.3115 (2)	2.42 (7)
O(5)	0.5478 (3)	0.1226 (2)	0.6082 (2)	3.81 (6)	C(24)	0.8829 (3)	0.1635 (2)	0.3016 (2)	2.67 (7)
O(6)	0.7434 (3)	0.1189 (1)	0.6714 (2)	3.63 (6)	C(25)	0.9300 (4)	0.1444 (2)	0.2482 (2)	3.80 (9)
O(7)	0.5862 (2)	0.1719 (1)	0.4578 (1)	2.47 (5)	C(26)	0.9512 (5)	0.1898 (3)	0.2042 (2)	4.3 (1)
O(8)	0.4494 (3)	0.3611 (2)	0.4956 (2)	3.99 (7)	C(27)	0.9288 (5)	0.2510 (3)	0.2136 (2)	3.95 (9)
O(9)	0.4745 (3)	0.3612 (2)	0.3800 (2)	4.10 (7)	C(28)	0.8801 (4)	0.2693 (2)	0.2686 (2)	2.88 (8)
O(10)	0.7781 (2)	0.2834 (1)	0.3922 (1)	2.44 (5)	C(29)	0.7668 (6)	0.4233 (2)	0.4143 (3)	6.7 (1)
O(11)	0.7559 (3)	0.0796 (1)	0.3500 (2)	3.72 (6)	C(30)	0.7603 (8)	0.4851 (3)	0.4017 (4)	12.5 (2)
O(12)	0.9528 (3)	0.0961 (1)	0.4059 (2)	3.57 (6)	C(31)	0.7172 (9)	0.5221 (3)	0.4448 (5)	10.7 (2)
N(1)	0.9201 (3)	0.2885 (1)	0.5180 (2)	2.33 (6)	C(32)	0.6852 (7)	0.4974 (2)	0.4998 (4)	7.3 (2)
N(2)	0.6931 (3)	0.2033 (1)	0.5873 (2)	2.21 (6)	C(33)	0.6926 (5)	0.4354 (2)	0.5083 (3)	4.3 (1)
N(3)	0.5660 (3)	0.2762 (1)	0.4541 (2)	2.35 (6)	C(34)	0.6722 (4)	0.0395 (2)	0.4940 (2)	3.43 (9)
N(4)	0.8049 (3)	0.1808 (1)	0.4080 (2)	2.29 (6)	C(35)	0.6767 (5)	−0.0233 (2)	0.5004 (3)	4.7 (1)
N(5)	0.7349 (3)	0.3984 (2)	0.4662 (2)	3.23 (7)	C(36)	0.7799 (5)	−0.0494 (2)	0.5303 (3)	4.4 (1)
N(6)	0.7605 (3)	0.0760 (1)	0.5153 (2)	2.64 (6)	C(37)	0.8700 (5)	−0.0128 (2)	0.5523 (3)	4.4 (1)
C(1)	0.9687 (3)	0.2367 (2)	0.5413 (2)	2.18 (7)	C(38)	0.8577 (4)	0.0499 (2)	0.5445 (3)	3.64 (9)
C(2)	1.0948 (3)	0.2422 (2)	0.5659 (2)	2.64 (7)	C(100)	0.5318 (7)	0.4913 (4)	0.6817 (4)	7.7 (2)*
C(3)	1.1338 (3)	0.3004 (2)	0.5578 (2)	2.91 (8)	C(101)	0.5466 (8)	0.4857 (5)	0.7444 (5)	8.5 (2)*
C(4)	1.2473 (4)	0.3172 (3)	0.5765 (3)	4.5 (1)	C(102)	0.4598 (9)	0.4710 (5)	0.7772 (5)	9.5 (2)*
C(5)	1.3218 (4)	0.2722 (3)	0.6042 (3)	5.1 (1)	C(103)	0.351 (1)	0.4571 (8)	0.7391 (7)	13.4 (4)*
C(6)	1.2840 (4)	0.2130 (3)	0.6133 (3)	4.8 (1)	C(104)	0.342 (1)	0.4610 (6)	0.6710 (6)	10.4 (3)*
C(7)	1.1691 (4)	0.1977 (2)	0.5952 (2)	3.44 (9)	C(105)	0.433 (1)	0.4803 (5)	0.6467 (5)	9.5 (2)*
C(8)	0.6829 (3)	0.2607 (2)	0.6063 (2)	2.11 (7)	C(200)	0.612 (1)	0.5251 (6)	0.1992 (6)	11.7 (3)*
C(9)	0.6346 (3)	0.2679 (2)	0.6678 (2)	2.28 (7)	C(201)	0.700 (1)	0.5311 (7)	0.1976 (7)	12.8 (4)*
C(10)	0.6076 (3)	0.2111 (2)	0.6922 (2)	2.56 (7)	C(202)	0.780 (1)	0.5734 (8)	0.2232 (8)	15.0 (5)*
C(11)	0.5577 (4)	0.2044 (2)	0.7476 (2)	3.27 (8)	C(203)	0.725 (1)	0.6152 (7)	0.2587 (7)	13.4 (4)*
C(12)	0.5348 (4)	0.2584 (2)	0.7792 (2)	3.9 (1)	C(204)	0.617 (1)	0.6101 (7)	0.2728 (7)	13.4 (4)*
C(13)	0.5634 (4)	0.3146 (2)	0.7570 (2)	3.9 (1)	C(205)	0.549 (2)	0.571 (1)	0.230 (1)	18.9 (7)*

[a] B values for anisotropically refined atoms are given in the form of the equivalent isotropic displacement parameter defined as $^1/_3[a^2a^{*2}B_{11} + b^2b^{*2}B_{22} + c^2c^{*2}B_{33} + 2ab(\cos\gamma)a^*b^*B_{12} + 2ac(\cos\beta)a^*c^*B_{13} + 2bc(\cos\alpha)b^*c^*B_{23}]$. Starred B values are for atoms that were refined isotropically.

of full-matrix least-squares refinement, a difference Fourier map indicated the presence of an ill-defined molecule of pyridine on a general position. The interstitial solvent molecule was eventually modeled as two interpenetrating rigid hexagons with bond lengths fixed at 1.395 Å. The total occupancy for the two groups was fixed at 1.0; the major orientation (atoms C(201)–C(206) refined to an occupancy of 0.66 (1). No attempt was made to determine which of the solvent atoms was the nitrogen of the pyridine ring. In the final stages of refinement, all of the atoms of the metal complex were given anisotropic temperature factors. Hydrogen atoms were used in calculated positions, "riding" 1.08 Å from the appropriate carbon atom (complex only).[12]

Other information pertinent to the data collection and structure solution is given in Table I. Positional and displacement parameters for **1** and **2** are given in Tables II and III, respectively. Selected bond distances and bond angles for **1** are given in Table IV, and those for **2** are given in Table V.

Results and Discussion

Observations on the Interconvertibility of 1 and 2. Perhaps one of the most striking features of this pair of compounds is the facile interconversion of **1** and **2** in solution leading to an equilibrium between a mononuclear and a dinuclear species. Since the compounds differ significantly in color, we were able to study this equilibrium using the visible spectrum. Unfortunately, the red dinuclear species **1** show an ill-defined maximum in the visible spectra, overshadowed by a tail from a strong absorption from the UV region, as shown in Figure 1. This precluded a quantification of it. For the spectroscopic studies, samples were prepared by dissolving crystals of **1** and **2** in neat pyridine at temperatures ranging from −20 to 78 °C. The solutions were brownish-red at lower temperatures and green at higher temperatures. At a given temperature, the spectrum was always the same regardless of which crystals were used to prepare the solution. However, the rates at which crystals dissolved varied greatly, with that of **1** being slower than that of **2**.

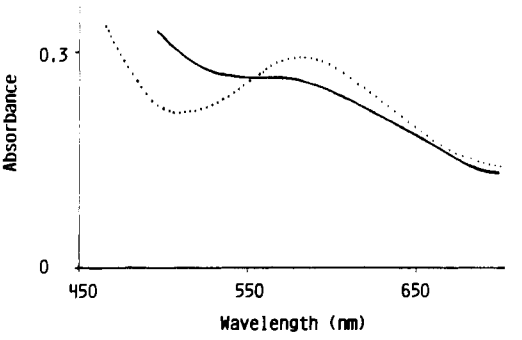

Figure 1. Visible absorption spectra for a pyridine solution of **2** at 25 °C (—) and 78 °C (···).

Figure 2 shows the behavior of the spectral maximum, in the visible region, when **1** and **2** were dissolved in pyridine. Practically no changes were observed after the temperature reached ca. 40 °C. The λ_{max} at 78 °C was 576 nm, regardless of the starting material used. The spectra were reproducible as the sample was allowed to cool. As long as oxygen was kept off the cells, the cycle could be repeated indefinitely indicating that there is a readily attainable and fully reversible equilibrium. One sample, maintained at 40 °C and monitored for 18 h, showed no change in the absorption maxima.

It is more remarkable that compounds **1** and **2** also interconvert in the solid state under certain circumstances. While in the mother liquor, they can be kept almost indefinitely. However, once they are isolated from solution, crystals of **2** are readily transformed to a brownish-red solid with the spectral properties of **1**. Crystals of **2** can be maintained out of solution for only a limited time.

Table III. Positional Parameters and *B* Values and Their Estimated Standard Deviations for $[Cr(Sac)_2(py)_3]\cdot 2py$[a]

atom	*x*	*y*	*z*	*B*, Å²
Cr	0.500	0.16209 (2)	0.250	2.44 (2)
S	0.57352 (7)	0.14786 (3)	0.00120 (7)	3.10 (2)
O(1)	0.5779 (2)	0.26453 (9)	0.1743 (2)	3.45 (6)
O(2)	0.4725 (2)	0.12627 (9)	−0.0724 (2)	3.83 (6)
O(3)	0.6610 (2)	0.1123 (1)	0.0459 (2)	4.48 (7)
N(1)	0.5601 (2)	0.1814 (1)	0.1116 (2)	2.79 (6)
N(2)	0.3400 (2)	0.1611 (1)	0.1248 (2)	2.94 (6)
N(3)	0.500	0.0727 (1)	0.250	3.2 (1)
C(1)	0.5806 (2)	0.2323 (1)	0.1007 (3)	2.68 (7)
C(2)	0.6041 (2)	0.2432 (1)	−0.0113 (3)	2.79 (7)
C(3)	0.6061 (3)	0.1993 (1)	−0.0749 (3)	2.98 (7)
C(4)	0.6273 (3)	0.2001 (2)	−0.1817 (3)	3.75 (9)
C(5)	0.6452 (3)	0.2475 (2)	−0.2236 (3)	4.2 (1)
C(6)	0.6415 (3)	0.2918 (2)	−0.1613 (3)	4.03 (9)
C(7)	0.6223 (3)	0.2908 (1)	−0.0536 (3)	3.45 (8)
C(8)	0.2666 (3)	0.1333 (1)	0.1514 (3)	3.67 (9)
C(9)	0.1600 (3)	0.1311 (2)	0.0762 (4)	4.5 (1)
C(10)	0.1271 (3)	0.1581 (2)	−0.0306 (4)	4.9 (1)
C(11)	0.2027 (4)	0.1867 (2)	−0.0576 (4)	5.2 (1)
C(12)	0.3062 (3)	0.1871 (2)	0.0209 (3)	4.05 (9)
C(13)	0.4609 (3)	0.0460 (1)	0.1471 (3)	3.73 (9)
C(14)	0.4597 (5)	−0.0066 (1)	0.1444 (4)	5.5 (1)
C(15)	0.500	−0.0326 (2)	0.250	6.9 (3)
C(101)	0.240 (1)	0.4770 (9)	0.191 (2)	17 (2)*
C(102)	0.260 (1)	0.4327 (9)	0.261 (2)	8.7 (5)*
C(103)	0.365 (1)	0.4181 (9)	0.326 (2)	20 (2)*
C(104)	0.450 (1)	0.4479 (9)	0.321 (2)	12.2 (9)*
C(105)	0.430 (1)	0.4923 (9)	0.251 (2)	12.7 (9)*
C(106)	0.325 (1)	0.5068 (9)	0.186 (2)	12.6 (9)*
C(201)	0.321 (1)	0.4037 (3)	0.297 (1)	11.7 (4)*
C(202)	0.369 (1)	0.4262 (3)	0.410 (1)	14.2 (5)*
C(203)	0.368 (1)	0.4793 (3)	0.422 (1)	21 (1)*
C(204)	0.319 (1)	0.5098 (3)	0.321 (1)	18.3 (8)*
C(205)	0.270 (1)	0.4873 (3)	0.208 (1)	14.0 (6)*
C(206)	0.271 (1)	0.4343 (3)	0.196 (1)	9.9 (3)*

[a] Anisotropically refined atoms are given in the form of the equivalent isotropic displacement parameter defined as $^1/_3[a^2a^{*2}B_{11} + b^2b^{*2}B_{22} + c^2c^{*2}B_{33} + 2ab(\cos\gamma)a^*b^*B_{12} + 2ac(\cos\beta)a^*c^*B_{13} + 2bc(\cos\alpha)b^*c^*B_{23}]$. Starred *B* values are for atoms that were refined isotropically.

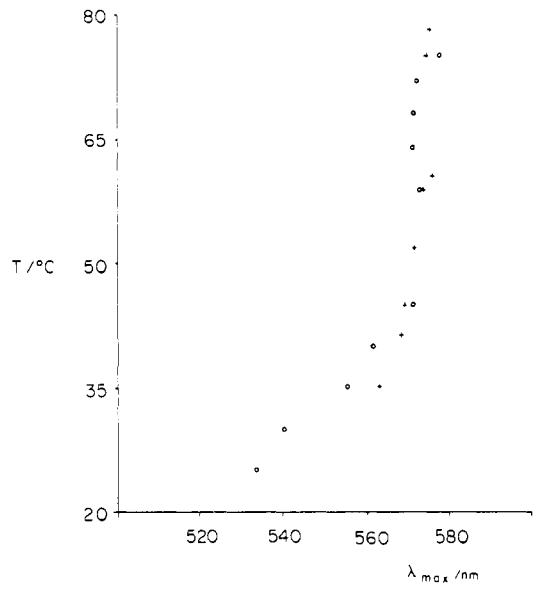

Figure 2. Variation of λ_{max} values of pyridine solutions of **1** and **2** at different temperatures. + indicates the solution was prepared from **1**, while O indicates the solution was prepared from **2**.

On the other hand, red crystals of **1** change, in a few hours, to green crystals if an atmosphere of pyridine is maintained in the flask, even if liquid pyridine is not in direct contact with the crystals. In the process, we observed several crystals which were approximately half red and the other half green. This phenomenon

Table IV. Selected Bond Distances (Å) and Bond Angles (deg) for $[Cr_2(Sac)_4(py)_2]\cdot 2py$[a]

Distances			
Cr(1)–Cr(2)	2.5911 (8)	Cr(2)–N(5)	2.265 (3)
Cr(1)–O(1)	2.021 (2)	O(1)–C(1)	1.257 (4)
Cr(1)–O(7)	1.985 (2)	O(4)–C(8)	1.261 (4)
Cr(1)–N(2)	2.087 (3)	O(7)–C(15)	1.253 (5)
Cr(1)–N(4)	2.098 (3)	O(10)–C(22)	1.249 (5)
Cr(1)–N(6)	2.267 (3)	N(1)–C(1)	1.324 (5)
Cr(2)–O(4)	2.005 (3)	N(2)–C(8)	1.326 (5)
Cr(2)–O(10)	2.005 (3)	N(3)–C(15)	1.343 (5)
Cr(2)–N(1)	2.111 (3)	N(4)–C(22)	1.330 (5)
Cr(2)–N(3)	2.093 (3)		
Angles			
Cr(2)–Cr(1)–O(1)	89.22 (7)	O(4)–Cr(2)–N(1)	90.3 (1)
Cr(2)–Cr(1)–O(7)	89.92 (8)	O(4)–Cr(2)–N(3)	88.4 (1)
Cr(2)–Cr(1)–N(2)	81.42 (8)	O(4)–Cr(2)–N(5)	91.3 (1)
Cr(2)–Cr(1)–N(4)	82.25 (9)	O(10)–Cr(2)–N(1)	88.1 (1)
Cr(2)–Cr(1)–N(6)	179.12 (8)	O(10)–Cr(2)–N(3)	92.8 (1)
O(1)–Cr(1)–O(7)	178.9 (1)	O(10)–Cr(2)–N(5)	90.0 (1)
O(1)–Cr(1)–N(2)	90.2 (1)	N(1)–Cr(2)–N(3)	163.2 (1)
O(1)–Cr(1)–N(4)	89.7 (1)	N(1)–Cr(2)–N(5)	97.9 (1)
O(1)–Cr(1)–N(6)	89.9 (1)	N(3)–Cr(2)–N(5)	98.8 (1)
O(7)–Cr(1)–N(2)	89.0 (1)	Cr(1)–O(1)–C(1)	120.3 (2)
O(7)–Cr(1)–N(4)	90.8 (1)	Cr(2)–O(4)–C(8)	119.5 (2)
O(7)–Cr(1)–N(6)	90.9 (1)	Cr(1)–O(7)–C(15)	120.3 (2)
N(2)–Cr(1)–N(4)	163.7 (1)	Cr(2)–O(10)–C(22)	121.0 (2)
N(2)–Cr(1)–N(6)	98.8 (1)	Cr(2)–N(1)–C(1)	122.7 (3)
N(4)–Cr(1)–N(6)	97.5 (1)	Cr(1)–N(2)–C(8)	123.8 (3)
Cr(1)–Cr(2)–O(4)	89.71 (8)	Cr(2)–N(3)–C(15)	123.0 (2)
Cr(1)–Cr(2)–O(10)	88.95 (8)	Cr(1)–N(4)–C(22)	122.4 (3)
Cr(1)–Cr(2)–N(1)	81.96 (9)	O(1)–C(1)–N(1)	124.7 (3)
Cr(1)–Cr(2)–N(3)	81.31 (9)	O(4)–C(8)–N(2)	124.1 (4)
Cr(1)–Cr(2)–N(5)	179.0 (1)	O(7)–C(15)–N(3)	123.9 (3)
O(4)–Cr(2)–O(10)	178.0 (1)	O(10)–C(22)–N(4)	124.4 (4)

[a] Numbers in parentheses are estimated standard deviations in the least significant digits.

Table V. Selected Bond Distances (Å) and Bond Angles (deg) for $[Cr(Sac)_2(py)_3]\cdot 2py$[a]

Distances			
Cr–N(1)	2.119 (3)	S–N(1)	1.632 (3)
Cr–N(2)	2.129 (2)	O(1)–C(1)	1.220 (4)
Cr–N(3)	2.335 (4)	N(1)–C(1)	1.372 (4)
S–O(2)	1.439 (2)	C(1)–C(2)	1.489 (5)
S–O(3)	1.439 (3)		
Angles			
N(1)–Cr–N(1′)	152.4 (1)	Cr–N(1)–S	131.6 (2)
N(1)–Cr–N(2)	91.5 (1)	Cr–N(1)–C(1)	116.4 (2)
N(1)–Cr–N(2′)	88.8 (1)	S–N(1)–C(1)	111.4 (2)
N(1)–Cr–N(3)	103.82 (7)	O(1)–C(1)–N(1)	123.0 (3)
N(2)–Cr–N(2′)	178.7 (1)	O(1)–C(1)–C(2)	124.7 (3)
N(2)–Cr–N(3)	89.34 (7)	N(1)–C(1)–C(2)	112.3 (3)
O(2)–S–O(3)	115.9 (1)	C(1)–C(2)–C(3)	112.1 (3)
O(2)–S–N(1)	110.6 (2)	S–C(3)–C(2)	107.7 (3)
O(3)–S–N(1)	110.9 (1)		

[a] Numbers in parentheses are estimated standard deviations in the least significant digits.

is reminiscent of the polymorphism exhibited by species such as $Ni(NCS)_2[P(CH_2CH_2CN)_3]_2$.[14] However, in the latter case the total composition of the crystal does not change.

Structure of 1. The structure of compound **1** is depicted in Figure 3. There is a nonrigorous 2-fold axis along the chromium-to-chromium bond. The saccharinate anions bridge the dichromium unit. This structure displays a great similarity to that of the THF adduct, with all common bond distances and angles being the same within the experimental error. The chromium-to-chromium bond length is extremely long, namely 2.5911 (8) Å. The average Cr to axial pyridine distance of 2.266 Å is longer than that of the Cr to axial THF (2.174 Å) by 0.093 Å,

(14) Foxman, B. M.; Goldberg, P. L.; Mazurek, H. *Inorg. Chem.* **1981**, *20*, 4368.

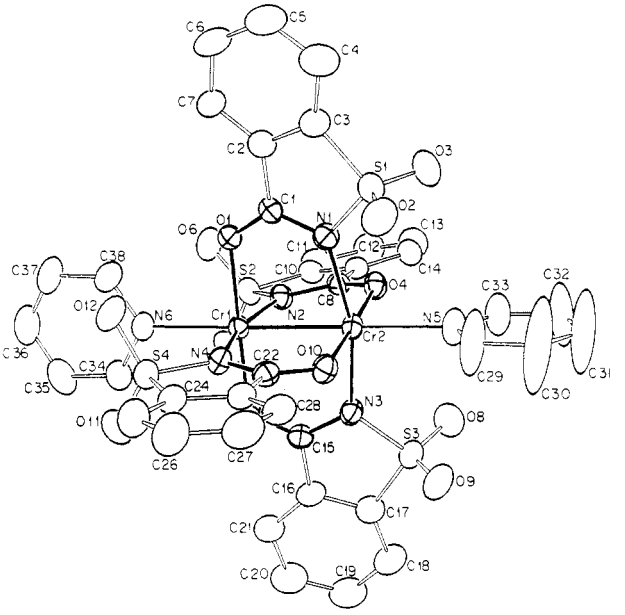

Figure 3. ORTEP drawing of the molecular structure of $[Cr_2(Sac)_4(py)_2]\cdot 2py$ (**1**), showing the atom-labeling scheme. All atoms are represented by their 50% probability ellipsoids.

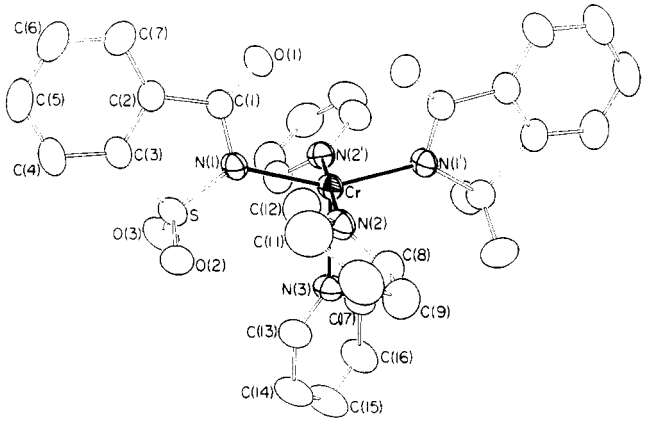

Figure 4. ORTEP plot of one molecule of $[Cr(Sac)_2(py)_3]\cdot 2py$ (**2**), showing the atom-labeling scheme. All atoms are represented by their 50% probability ellipsoids.

but there is exactly the same difference between the average of the remaining Cr–N bond lengths and the average of the remaining Cr–O bond lengths. This suggests that the longer axial distance is due mainly to the presence of a different atom rather than to any large change in bond strength.

As discussed in our earlier report,[3b] the long metal-to-metal bond is at least partly due to the high acidity of the parent saccharine ligand and the strong axial bond. We should also note that the geometry of the saccharinate anion also favors a longer Cr–Cr distance because the five-membered sulfonamide ring sets the preferred O–Cr and N–Cr bond directions along divergent lines.

Structure of 2. The structure of compound **2** is depicted in Figure 4. The chromium atom is coordinated by only five ligands (three pyridine molecules and two N-bonded saccharinate anions). It has a trigonal bipyramidal arrangement of atoms. The equatorial plane of the bipyramid is quite distorted, showing a Sac–Cr–Sac angle of 152.39 (9)° while the Sac–Cr–py angle is only 103.82 (7)°. This may be due to the greater steric demand of the larger saccharinate anion relative to that of the pyridine group. The axial py–Cr–py angle is essentially linear (178.7 (1)°). Except for the unique Cr–N bond in the equatorial plane of 2.335 (4) Å, the remaining bonds are very similar. The average bond length is 2.124 Å. This is only slightly longer than the one found on the dinuclear species and is close to the value of 2.113 (3) Å found in $[Cr(py)_4(PF_5)_2]$.[15]

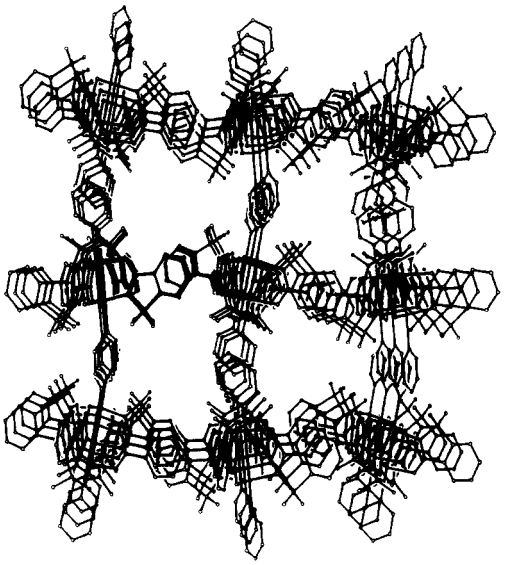

Figure 5. ORTEP drawing of the crystal packing of **1** viewed down *c*, from which the interstitial pyridine molecules have been omitted.

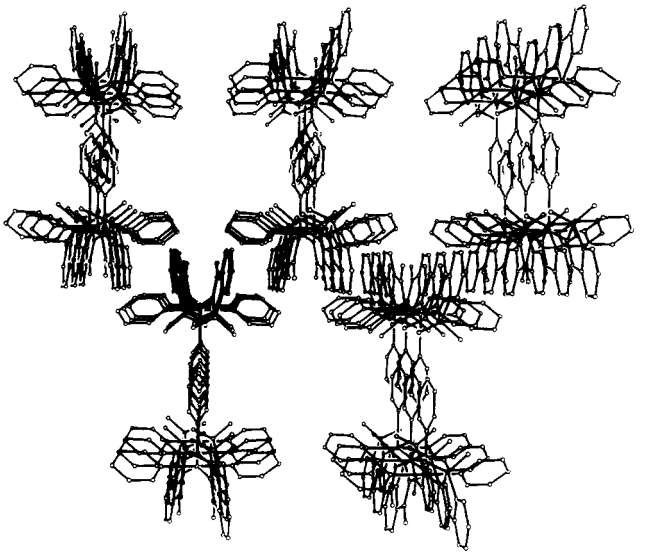

Figure 6. ORTEP plot of the crystal packing of **2**, viewed down *c*, from which the interstitial pyridine molecules have been omitted.

To our knowledge, the mononuclear compound **2** is the first compound to be structurally characterized by a diffraction study in which there is a trigonal bipyramidal arrangement of atoms about Cr^{II}. The only other five-coordinated compound structurally characterized, $(\eta^1\text{-}C_4H_4N)_2Cr(py)_3$,[5] has the square-pyramidal structure.

Structural Relationship of 1 and 2. Figures 5 and 6 show ORTEP drawings of the packing of the molecules, viewed down the *c* axis for compounds **1** and **2**, respectively. In both cases the interstitial pyridine molecules have been omitted. The drawings thus show long channels, along which the nonbonded pyridine molecules presumably can move and provide a path for the interconversion of the crystalline forms. Also, as seen from Figures 3 and 4, the five-coordinate mononuclear compound **2** has a geometry around the metal atom that is very close to that in the parent dinuclear species **1**. It is clear from the molecular drawing of **1** that, for each of the two chromium atoms, the arrangement of the two N-bonded saccharinate groups and the axial pyridine molecule is essentially the same as that of the ligands at the equatorial plane of the bipyramid that occurs in the molecule of **2**. The two remaining pyridine molecules, located at the apical positions of the bipyramid, are occupying the position of the O-bonded sac-

(15) Fochi, G.; Strähle, J.; Gingl, F. *Inorg. Chem.* **1991**, *30*, 4669.

charinate groups in molecule **1**. Even the angles formed by most of the related atoms are similar in **1** and **2**. All these factors contribute to the relatively easy interconversion of the two compounds in the solid state.

Acknowledgment. We are grateful to the Vicerrectoría de Investigación, UCR (Grant No. 115-87-516), for support of work at the University of Costa Rica and to the National Science Foundation for support of work at Texas A&M University.

Supplementary Material Available: For structures **1** and **2**, complete tables of crystal data, bond distances and angles, general displacement parameters, and positional parameters of calculated hydrogen atoms (18 pages); tables of observed and calculated structure factors (40 pages). Ordering information is given on any current masthead page.

Contribution from the Department of Chemistry and Laboratory for Molecular Structure and Bonding, Texas A&M University, College Station, Texas 77843

Compounds Containing Linked Multiply-Bonded Dimetal Units. 2. An Antiferromagnetic Compound Containing Infinite Chains of $Ru_2(O_2CR)_4^+$ Units Linked by Bridging Phenazine Molecules

F. Albert Cotton,* Youngmee Kim, and Tong Ren

Received January 24, 1992

The polymeric $[Ru_2(O_2CC_2H_5)_4(phz)]BF_4$ was prepared by reaction of $[Ru_2(O_2CC_2H_5)_4(H_2O)_2]BF_4$ with phz (phenazine). Crystals of $[Ru_2(O_2CC_2H_5)_4(phz)]BF_4$ were obtained by a diffusion technique in which a dichloromethane solution of $[Ru_2(O_2CC_2H_5)_4(H_2O)_2]BF_4$ was carefully layered by a benzene solution containing an excess amount of phz. The compound has been characterized by X-ray crystallography and magnetic susceptibility measurements from ca. 2 to ca. 300 K. The space group is $P\bar{1}$, and there are two formula units per unit cell with a = 11.669 (5) Å, b = 14.471 (2) Å, c = 8.963 (1) Å, α = 103.96 (1)°, β = 96.743 (2)°, and γ = 70.237 (2)°. The phz ligands connect the dinuclear species into kinked chains that all run parallel to the 111 direction. There are two crystallographically independent $Ru_2(O_2CC_2H_5)_4^+$ cations with Ru(1)–Ru(1)′ = 2.2756 (6) Å, Ru(2)–Ru(2)′ = 2.2747 (7) Å, Ru(1)–N(1) = 2.436 (4) Å, and Ru(2)–N(2) = 2.443 (5) Å. The BF_4^- ions occupy general positions between the chains. The compound is antiferromagnetic with a magnetic moment of ca. 4.3 μ_B at 300 K that tends toward zero as 0 K is approached (1.72 μ_B at 2.7 K).

Introduction

A number of compounds containing $Ru_2(O_2CR)_4^+$ moieties are known, and in general they are well characterized.[1,2] They have three unpaired electrons, and it is generally accepted that this results from an electron configuration $\sigma^2\pi^4\delta^2(\delta^*\pi^*)^3$, where we use the symbol $(\delta^*\pi^*)^3$ to denote the fact that the δ^* and π^* orbitals are nearly degenerate. In several cases,[2] $Ru_2(O_2CR)_4X$ (X = Cl, Br) compounds have been found to have chain structures where shared axial halide ions link the $Ru_2(O_2CR)_4^+$ ions in either linear or kinked chains. The butyrate has been studied magnetically,[1a,c] and it was concluded that magnetic coupling of the Ru_2^{5+} units along the chain (one-dimensional antiferromagnetism, ODAFM) was not occurring.

We undertook the work described here to see if we could find a bridging ligand that would cause the formation of infinite chains displaying ODAFM. In our first effort, we employed the aromatic diamine phenazine (I) as the linking ligand and we have obtained a compound of the desired type, $[Ru_2(O_2CC_2H_5)_4(phz)]BF_4$, where we use phz to represent phenazine.

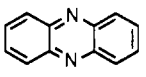

I

(1) (a) Cotton, F. A.; Pedersen, E. *Inorg. Chem.* **1975**, *14*, 388. (b) Clark, R. J. H.; Ferris, L. H. *Inorg. Chem.* **1981**, *20*, 2759. (c) Telser, J.; Drago, R. S. *Inorg. Chem.* **1984**, *23*, 3114. (d) Miskowski, V. M.; Gray, H. B. *Inorg. Chem.* **1988**, *27*, 2501.

(2) (a) Bennett, M. J.; Caulton, K. G.; Cotton, F. A. *Inorg. Chem.* **1969**, *8*, 1. (b) Bino, A.; Cotton, F. A.; Felthouse, T. R. *Inorg. Chem.* **1979**, *18*, 2599. (c) Togano, T.; Mukaida, M.; Nomura, T. *Bull. Chem. Soc. Jpn.* **1980**, *53*, 2085. (d) Martin, D. S.; Newman, R. A.; Vlasnik, L. M. *Inorg. Chem.* **1980**, *19*, 3404. (e) Kimura, T.; Sakurai, T.; Shima, M.; Togano, T.; Mukaida, M.; Nomura, T. *Bull. Chem. Soc. Jpn.* **1982**, *55*, 3927. (f) Cotton, F. A.; Matusz, M.; Zhong, B. *Inorg. Chem.* **1988**, *27*, 4368.

Table I. Crystal Data for $[Ru_2(Pro)_4(phz)]BF_4$

formula	$Ru_2O_8C_{24}H_{28}N_2BF_4$	Z	2
		d_{calc}, g/cm^3	1.831
fw	761.4	μ(Mo Kα), cm^{-1}	11.471
space group	$P\bar{1}$ (No. 2)	radiation monochromated in incident beam (λ, Å)	Mo Kα (0.710 73)
a, Å	11.669 (5)	temp, °C	20
b, Å	14.471 (2)	transm factors: max; min	1.00; 0.86
c, Å	8.963 (1)		
α, deg	103.96 (1)	R^a	0.045
β, deg	96.743 (2)	R_w^b	0.062
γ, deg	70.237 (2)		
V, Å^3	1381 (1)		

$^a R = \sum||F_o| - |F_c||/\sum|F_o|$. $^b R_w = [\sum w(|F_o| - |F_c|)^2/\sum w|F_o|^2]^{1/2}$; $w = 1/\sigma^2(|F_o|)$.

Experimental Section

The starting material, $Ru_2(O_2CC_2H_5)_4Cl$, was prepared by using a literature procedure.[3] Phenazine was purchased from Aldrich Chemical Co. and used as received.

Preparation of $[Ru_2(O_2CC_2H_5)_4(H_2O)_2]BF_4$. An aqueous solution of $Ru_2(O_2CC_2H_5)_4Cl$ was absorbed on a cation-exchange column (Dowex 50W-X1) and eluated with 0.5 M $NaBF_4$. Evaporation of the eluate gave the brown product and the excess $NaBF_4$. The excess $NaBF_4$ was removed from the product by recrystallization from methanol several times. IR (Nujol mull, cm^{-1}): 3300–3600 (broad), 1300 m, 1000–1150 (several bands), 810 w, 720 m, 635 w, 450 w. UV–vis (CH_2Cl_2 solution; λ, nm (ϵ, M^{-1} cm^{-1})): 423 (330).

Preparation of $[Ru_2(O_2CC_2H_5)_4(phz)]BF_4$. A 154-mg sample (0.25 mmol) of $[Ru_2(O_2CC_2H_5)_4(H_2O)_2]BF_4$ was suspended in 10 mL of benzene. A solution of phenazine (phz), 90 mg (0.5 mmol) in 10 mL of benzene, was added to this suspension. The reaction mixture was refluxed for 3 h, and the color of the reaction mixture changed from brown to reddish brown. The precipitate was collected, washed with benzene several times to remove the excess phenazine, and dried under vacuum.

(3) Stephenson, T. A.; Wilkinson, G. *J. Inorg. Nucl. Chem.* **1966**, *28*, 2285.

0020-1669/92/1331-2723$03.00/0